

Phenomenology of the three-flavor PNJL model and thermal strange quark production

Hung-Ming Tsai and Berndt Müller

Department of Physics, Duke University, Durham, NC 27708, USA

E-mail: ht25@phy.duke.edu, mueller@phy.duke.edu

Abstract. We study the temperature dependence of the adjoint Polyakov loop and its implication for the momentum spectrum of gluons in the mean-field approximation. This allows us to calculate the contribution of the thermal (transverse) gluons to the thermodynamic pressure. As an application, we evaluate the rates for the strange quark pair-production processes $q\bar{q} \rightarrow s\bar{s}$ and $gg \rightarrow s\bar{s}$ as functions of temperature including thermal effects on quark deconfinement and chiral symmetry breaking.

1. Introduction

The increased abundance of particles containing strange quarks in the spectrum of emitted hadrons, especially hyperons, was proposed by Hagedorn and Rafelski [1] as a signal for the formation of quark matter in relativistic heavy ion collisions. Soon afterwards, the enhanced pair production of strange quarks required for the saturation of strange quark phase space was predicted to occur as an effect of quark and gluon deconfinement [2, 3, 4, 5]. The predicted enhancement has been observed in many experiments (see, in particular: [6, 7]). The parameter γ_s , describing the degree of saturation of the phase space of strange hadrons, has been determined by thermal chemical fits to the abundances of hadrons emitted in collisions between two ^{197}Au nuclei at center-of-mass energies of 200 GeV/nucleon at the Relativistic Heavy Ion Collider (RHIC). Values for this parameter obtained in such fits range from $\gamma_s = 1.03 \pm 0.04$ [8] to $\gamma_s = 2.00 \pm 0.02$ [9].

It is important to understand how the dynamics of deconfinement and chiral symmetry affects the prediction of production of the strange quarks and therefore its enhancement. The recently developed three-flavor PNJL model [10, 11] has made such a study possible. In the present work we explore the effect of the temperature dependence of the Polyakov loops and chiral condensates on the strange quark production. Our article is structured as follows. After stating the basic equations of the PNJL model, including the thermal quark and antiquark distribution functions, we obtain an explicit fit for the temperature dependence of the effective action of the Polyakov loop in mean-field theory. We confirm that this action satisfies the scaling of the thermal averages of the Polyakov loop in different color representations by their Casimir operator. We then calculate the temperature dependence of the thermal average of the adjoint Polyakov loop, the thermal distribution function of transverse gluons and the contribution of transverse gluons to the thermodynamic potential.

Finally, we calculate the temperature dependence of the pair-production rate of strange quarks using the Polyakov loop-suppressed quark and gluon distribution functions. With the aid of the PNJL model, we identify the temperature where the gluonic contribution to the production rate becomes dominant. The cross-over of the contributions from light quarks and gluons is a novel phenomenon which does not exist in the traditional approach to strange quark-pair production based on perturbation theory [2].

2. The PNJL model

The phase transformations of QCD matter due to deconfinement and chiral symmetry restoration have been combined in one theoretical framework, which is the Nambu-Jona-Lasinio model with the Polyakov loop (PNJL model) [12, 13]. The Polyakov loop in

color-SU(3) representation r is defined as

$$L_r = \mathcal{P} \exp \left(ig \int_0^{1/T} d\tau A_4(\mathbf{x}, \tau) \right), \quad (1)$$

where \mathcal{P} denotes that the exponential is path-ordered, T denotes the temperature and $A_4(\mathbf{x}, \tau)$ is the temporal component of the SU(3) gauge field in representation r . In particular, L_3 and L_8 denote the Polyakov loops in the fundamental and adjoint representations, respectively. The traces of the Polyakov loops are defined as

$$\ell_3 = N_c^{-1} \text{tr}_F L_3, \quad \bar{\ell}_3 = N_c^{-1} \text{tr}_F L_3^\dagger, \quad (2)$$

$$\ell_8 = (N_c^2 - 1)^{-1} \text{tr}_A L_8, \quad (3)$$

where tr_F and tr_A denote the color traces in the fundamental and adjoint representation, respectively. Note that the dependence of L_r , L_r^\dagger , ℓ_r and $\bar{\ell}_r$ on the spatial coordinate \mathbf{x} is suppressed in (1)-(3). With the above definitions, the Lagrangian of the three flavor PNJL model is [11]

$$\begin{aligned} \mathcal{L} = & \bar{\psi} (i\boldsymbol{\gamma} \cdot D - \hat{m}_0) \psi - \mathcal{U}(\ell_3, \bar{\ell}_3; T) \\ & + \frac{g_S}{2} \sum_{a=0}^8 \left[(\bar{\psi} \lambda^a \psi)^2 + (\bar{\psi} i\gamma_5 \lambda^a \psi)^2 \right] \\ & + g_D \left[\det \bar{\psi} (1 - \gamma_5) \psi + h.c. \right], \end{aligned} \quad (4)$$

where $D_\mu = \partial_\mu - g\delta_{\mu 4} A_4$ is the gauge-covariant derivative, $\mathcal{U}(\ell_3, \bar{\ell}_3; T)$ is the effective potential for the Polyakov loop and the three-flavor current quark mass matrix $\hat{m}_0 = \text{diag}(m_{u,0}, m_{d,0}, m_{s,0})$. In the limit of isospin symmetry, $m_{u,0} = m_{d,0} = m_{q,0}$. In the mean-field approximation, the chiral condensates and the thermal averages of the Polyakov loops are the order parameters of the phase transition [11, 13]. Note that, in the mean-field approximation, the thermal average of the Polyakov loop is independent of the spatial coordinate \mathbf{x} .

To encode the features of the temperature dependence of the effective potential $\mathcal{U}(\ell_3, \bar{\ell}_3; T)$, the nonperturbative contribution to the gluon thermodynamic potential per unit volume is assumed to be of the following form [11]:

$$\begin{aligned} \Omega_g^{\text{NP}} = & -bT \left\{ 54 \exp \left(-\frac{a}{T} \right) \langle \ell_3 \rangle \langle \bar{\ell}_3 \rangle \right. \\ & \left. + \ln \left[1 - 6 \langle \ell_3 \rangle \langle \bar{\ell}_3 \rangle - 3 \left(\langle \ell_3 \rangle \langle \bar{\ell}_3 \rangle \right)^2 + 4 \left(\langle \ell_3 \rangle^3 + \langle \bar{\ell}_3 \rangle^3 \right) \right] \right\}, \end{aligned} \quad (5)$$

where $\langle \ell_3 \rangle$ and $\langle \bar{\ell}_3 \rangle$ are the thermal averages of the Polyakov loops in (2). Standard values for the parameters in (4) and (5) are $a = 0.664 \text{ GeV}$, $b = 0.03\Lambda^3$, $g_S = 3.67\Lambda^{-2}$, $g_D = -9.29\Lambda^{-5}$ and $\Lambda = 0.6314 \text{ GeV}$ [11]. Moreover, it is straightforward to obtain the quark partition function from the quark Lagrangian, yielding the quark grand canonical thermodynamic potential per unit volume [11]:

$$\begin{aligned} \Omega_q = & -2T \left\langle \sum_{f=u,d,s} \int \frac{d^3k}{(2\pi)^3} \left\{ \text{tr}_F \ln \left[1 + L_3 \exp \left(\frac{-(E_f(\mathbf{k}) - \mu_f)}{T} \right) \right] \right. \right. \\ & \left. \left. + \text{tr}_F \ln \left[1 + L_3^\dagger \exp \left(\frac{-(E_f(\mathbf{k}) + \mu_f)}{T} \right) \right] \right\} \right\rangle \end{aligned}$$

$$-6 \sum_{f=u,d,s} \int \frac{d^3k}{(2\pi)^3} E_f(\mathbf{k}) \theta(\Lambda^2 - |\mathbf{k}|^2), \quad (6)$$

where $E_f(\mathbf{k}) = (|\mathbf{k}|^2 + m_f^2)^{1/2}$ are the single-particle energies, and m_f and μ_f are the constituent mass and chemical potential of the quark with flavor f . The constituent quark masses are related to the current masses and the chiral condensates by

$$m_q = m_{q,0} - 2g_S \langle \bar{q}q \rangle - 2g_D \langle \bar{q}q \rangle \langle \bar{s}s \rangle, \quad (q = u, d) \quad (7)$$

$$m_s = m_{s,0} - 2g_S \langle \bar{s}s \rangle - 2g_D \langle \bar{q}q \rangle^2, \quad (8)$$

where $\langle \bar{u}u \rangle = \langle \bar{d}d \rangle$ and $m_{u,0} = m_{d,0}$. Furthermore, in the mean-field approximation, the quark condensate contribution to the thermodynamic potential per unit volume is [11]

$$\Omega_{\text{cond}} = g_S \left(2\langle \bar{q}q \rangle^2 + \langle \bar{s}s \rangle^2 \right) + 4g_D \langle \bar{q}q \rangle^2 \langle \bar{s}s \rangle. \quad (9)$$

In the present article, the parameters are chosen as follows: $m_{q,0} = 0.0055$ GeV, $m_{s,0} = 0.1357$ GeV. The vacuum quark condensates are $\langle \bar{q}q \rangle_0 = (-0.246 \text{ GeV})^3$ and $\langle \bar{s}s \rangle_0 = (-0.267 \text{ GeV})^3$ [11].

In the mean-field approximation, one easily derives the temperature dependence of the chiral condensates $\langle \bar{q}q \rangle$ and $\langle \bar{s}s \rangle$ as well as the thermal averages of the Polyakov loops in the fundamental representation, i.e. $\langle \ell_3 \rangle$ and $\langle \bar{\ell}_3 \rangle$ [11]. Furthermore, it is straightforward to derive from (6) the color-averaged distribution functions for q and \bar{q} [14]:

$$f_q(k) = \frac{\langle \ell_3 \rangle \lambda_+ + 2\langle \bar{\ell}_3 \rangle \lambda_+^2 + \lambda_+^3}{1 + 3\langle \ell_3 \rangle \lambda_+ + 3\langle \bar{\ell}_3 \rangle \lambda_+^2 + \lambda_+^3}, \quad (10)$$

$$f_{\bar{q}}(k) = \frac{\langle \bar{\ell}_3 \rangle \lambda_- + 2\langle \ell_3 \rangle \lambda_-^2 + \lambda_-^3}{1 + 3\langle \bar{\ell}_3 \rangle \lambda_- + 3\langle \ell_3 \rangle \lambda_-^2 + \lambda_-^3}, \quad (11)$$

where we introduced the abbreviations $\lambda_{\pm} = \exp[-(|\mathbf{k}|^2 + m_q^2)^{1/2} \mp \mu]/T$ and chose an isospin-independent chemical potential for the light quarks: $\mu = \mu_u = \mu_d$. Equations (10) and (11) are obtained by assuming the Weiss mean-field approximation [11]. In Appendix A, we discuss several Polyakov-loop averaging procedures for evaluating the quark thermodynamic potential and thereby comparing the quark distribution functions derived from these different averaging procedures. In the following, we will consider the choice $\mu = 0.1$ GeV. These distribution functions are to be used in the study of the strange quark pair-production rates due to the process $q\bar{q} \rightarrow s\bar{s}$.

3. Adjoint Polyakov loop and gluon distribution function

In order to describe the process $gg \rightarrow s\bar{s}$, we also need to calculate the adjoint Polyakov loop and study how it affects the gluon distribution function. Starting from the Yang-Mills Lagrangian $\mathcal{L}_g = -(1/4)F_{\mu\nu}^a F^{a,\mu\nu}$, it is straightforward to write down the gluon partition function for the transverse gluons, and obtaining the perturbative contribution

to the gluon thermodynamic potential per unit volume [15, 16],

$$\begin{aligned} \Omega_g^P &= 2T \left\langle \int \frac{d^3k}{(2\pi)^3} \text{tr}_A \ln [1 - L_8 \exp(-|\mathbf{k}|/T)] \right\rangle \\ &\quad + 8 \int \frac{d^3k}{(2\pi)^3} |\mathbf{k}| \theta(\Lambda^2 - |\mathbf{k}|^2). \end{aligned} \quad (12)$$

Because $A_4(\mathbf{x}, \tau)$ is assumed to be independent of the spatial coordinate \mathbf{x} in the mean-field approximation, the Polyakov loop in the fundamental representation can be gauge rotated to diagonal form, $L_3 = \text{diag}(e^{i\phi_1}, e^{i\phi_2}, e^{i\phi_3})$, with $\phi_3 = -(\phi_1 + \phi_2)$. Therefore,

$$\ell_3 = (\bar{\ell}_3)^* = \frac{1}{3} [\exp(i\phi_1) + \exp(i\phi_2) + \exp(-i(\phi_1 + \phi_2))]. \quad (13)$$

In the same gauge, L_8 can be expressed in terms of the eigenvalues of L_3 [15]:

$$L_8 = \text{diag} \left(1, 1, e^{i\phi_{31}}, e^{i\phi_{13}}, e^{i\phi_{23}}, e^{i\phi_{32}}, e^{i\phi_{21}}, e^{i\phi_{12}} \right), \quad (14)$$

where $\phi_{jk} = \phi_j - \phi_k$. Thus,

$$\ell_8 = \frac{1}{8} \text{tr}_A L_8 = \frac{1}{4} \left(1 + \sum_{j<k} \cos \phi_{jk} \right). \quad (15)$$

Inserting (14) into (12) and after some algebraic transformations, the color-averaged gluon distribution function is obtained as

$$f_g(k) = \frac{1}{8} \sum_{n=1}^{\infty} \langle \text{tr}_A L_8^n \rangle \exp(-n|\mathbf{k}|/T), \quad (16)$$

where

$$\text{tr}_A L_8^n = 2 \left[1 + \sum_{j<k} \cos n\phi_{jk} \right]. \quad (17)$$

The remaining task is to evaluate $\langle \text{tr}_A L_8^n \rangle$. In order to do so, we need to specify the full distribution of eigenvalues of the Polyakov loop, i. e. the distribution of phases ϕ_i . The thermal average of any function of the eigenvalues of the Polyakov loop, $F(\phi_1, \phi_2)$, is defined as

$$\langle F(\phi_1, \phi_2) \rangle = \frac{\int_0^{2\pi} d\phi_1 \int_0^{2\pi} d\phi_2 H(\phi_1, \phi_2) W(\phi_1, \phi_2; T) F(\phi_1, \phi_2)}{\int_0^{2\pi} d\phi_1 \int_0^{2\pi} d\phi_2 H(\phi_1, \phi_2) W(\phi_1, \phi_2; T)}, \quad (18)$$

where $H(\phi_1, \phi_2)$ is the SU(3) Haar measure, the weight function $W(\phi_1, \phi_2; T)$ denotes the distribution of eigenvalues of the Polyakov loop. The Haar measure for the SU(3) symmetry group is given by $H(\phi_1, \phi_2) = \prod_{j<k} \sin^2(\phi_{jk}/2)$. Since $\phi_3 = -(\phi_1 + \phi_2)$, the integration in (18) only goes over ϕ_1 and ϕ_2 . A suitable choice of the weight function is a crucial step in evaluating $\langle F(\phi_1, \phi_2) \rangle$. We follow Gocksch and Ogilvie [17] and Gupta *et al.* [18] in choosing a weight function of the form

$$W(\phi_1, \phi_2; T) = \exp(6d\beta_3 \langle \ell_3 \rangle \text{Re}(\ell_3)), \quad (19)$$

where $d = 3$ and $\beta_3(T)$ is a fit parameter depending on temperature. The particular form (19) is suggested by the strong coupling expansion of the gauge theory. We note that $\exp[-\mathcal{U}(\ell_3, \bar{\ell}_3; T)/(bT)]$ and $H(\phi_1, \phi_2)W(\phi_1, \phi_2)$ have a corresponding structure

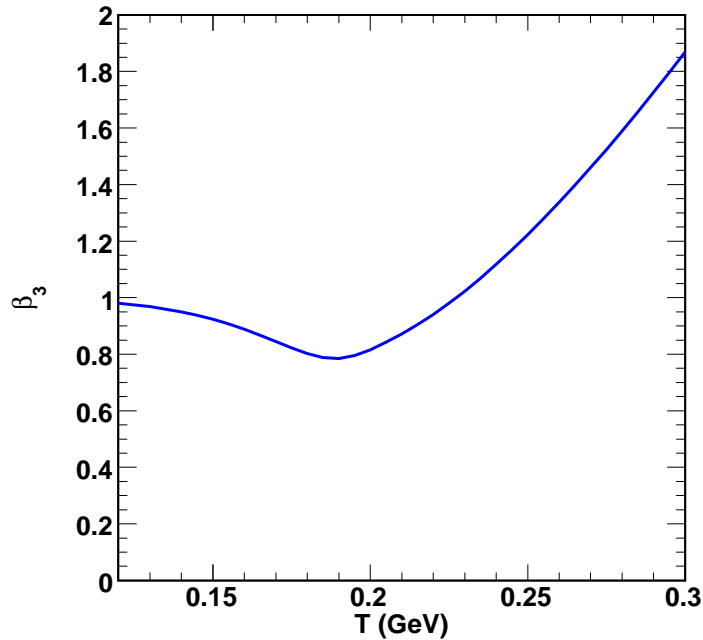


Figure 1. The fit parameter β_3 as a function of temperature.

expressed in terms of the eigenvalues of the fundamental Polyakov loops, as can be seen from assuming $\mathcal{U}(\ell_3, \bar{\ell}_3; T)$ to be in the form of (5) with $\langle \ell_3 \rangle$ and $\langle \bar{\ell}_3 \rangle$ replaced by ℓ_3 and $\bar{\ell}_3$ respectively. Starting from (19) and inserting the known values of $\langle \ell_3 \rangle$ into (18), the temperature dependence of β_3 can be solved numerically, as shown in figure 1. We now have obtained an explicit expression for $W(\phi_1, \phi_2)$ at each temperature.

We note that the temperature corresponding to the minimum of β_3 in figure 1 coincides with the critical temperature of the deconfinement phase transition in the mean-field approximation. In their investigation of the gluonic contribution to the thermodynamic potential of the PNJL model, Megias *et al.* [16] used a weight function of similar form as (19), but did not make the mean-field approximation. They determined the parameter β_3 from the empirical relation between string tension and the deconfinement temperature of the pure gauge theory. Here, we have determined β_3 by imposing a self-consistency condition on the expectation value of the fundamental Polyakov loop.

With the weight function (19), equation (18) allows us to evaluate the thermal average of the adjoint Polyakov loop $\langle \ell_8 \rangle$ and thus the gluon distribution function $f_g(k)$. The temperature dependence of the quark condensates and the thermal averages of the Polyakov loop $\langle \ell_3 \rangle$, $\langle \bar{\ell}_3 \rangle$ were first calculated in [11], as well as the temperature dependence of $\langle \ell_8 \rangle$ are shown in figure 2. Furthermore, the temperature dependence of the constituent masses of quarks are obtained from (7) and (8), as shown in figure 3.

To verify the validity of $\langle \ell_8 \rangle$ obtained by this procedure, we check its consistency with the Casimir scaling of the thermal averages of the Polyakov loop observed in lattice

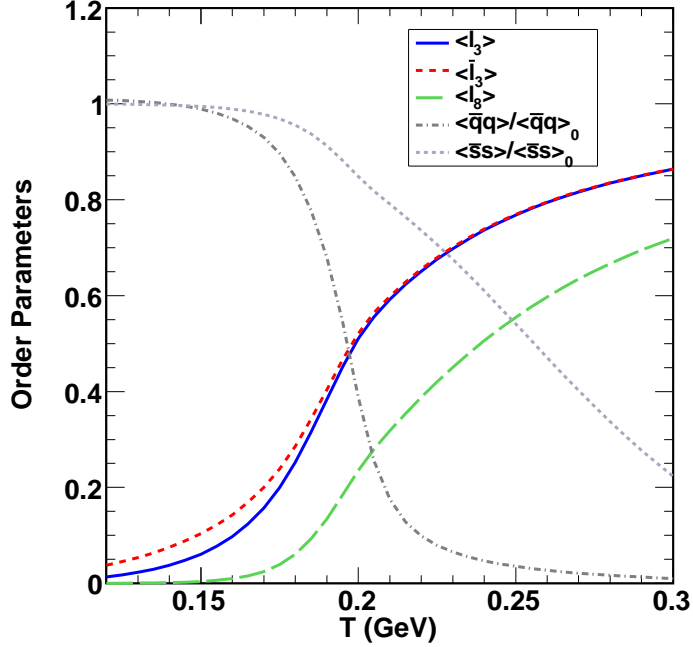


Figure 2. The temperature dependence of the order parameters, ℓ_3 , $\bar{\ell}_3$, ℓ_8 , $\langle \bar{q}q \rangle / \langle \bar{q}q \rangle_0$ and $\langle \bar{s}s \rangle / \langle \bar{s}s \rangle_0$. The values of the vacuum quark condensates are $\langle \bar{q}q \rangle_0 = (-0.246 \text{ GeV})^3$ and $\langle \bar{s}s \rangle_0 = (-0.267 \text{ GeV})^3$.

QCD [18, 19]. Casimir scaling refers to a relation, valid for all temperatures, between the thermal averages of the Polyakov loop in different representations r of color-SU(3) of the form

$$\langle \ell_r \rangle = \langle \ell_3 \rangle^{d_r}, \quad (20)$$

where $d_r = C_2(r)/C_2(3)$ and $C_2(r)$ denotes the eigenvalue of the quadratic Casimir operator in representation r . For the adjoint representation, $d_8 = C_2(8)/C_2(3) = 9/4$ and thus $\langle \ell_8 \rangle = \langle \ell_3 \rangle^{9/4}$. Figure 4 shows our results for $\langle \ell_8 \rangle$, together with $\langle \ell_3 \rangle^{9/4}$, as function of $\langle \ell_3 \rangle$. As can be seen, the values of $\langle \ell_8 \rangle$ and $\langle \ell_3 \rangle^{9/4}$ show a good agreement with Casimir scaling (20) for temperatures T ranging from 0.12 GeV to 0.30 GeV.

By numerically evaluating $\langle \text{tr}_A L_8^n \rangle$ for each power n and as a function of temperature T , the gluon distribution function can now be obtained from (16). The ratios $f_q(k)/f_{\text{FD}}(k)$ and $f_g(k)/f_{\text{BE}}(k)$ are plotted in figure 5, where f_{FD} and f_{BE} are the free Fermi-Dirac and Bose-Einstein distributions, respectively, with the constituent quark mass m_q in (7) and $\mu = 0.1 \text{ GeV}$. When T is near T_c , gluon is more strongly suppressed than quarks in spite of the additional effect of chiral symmetry breaking on the constituent quark mass m_q . Furthermore, we evaluate the quark, antiquark, net quark and gluon number densities by

$$n_q = n_u + n_d = 4N_c \int \frac{d^3k}{(2\pi)^3} f_q(k), \quad (21)$$

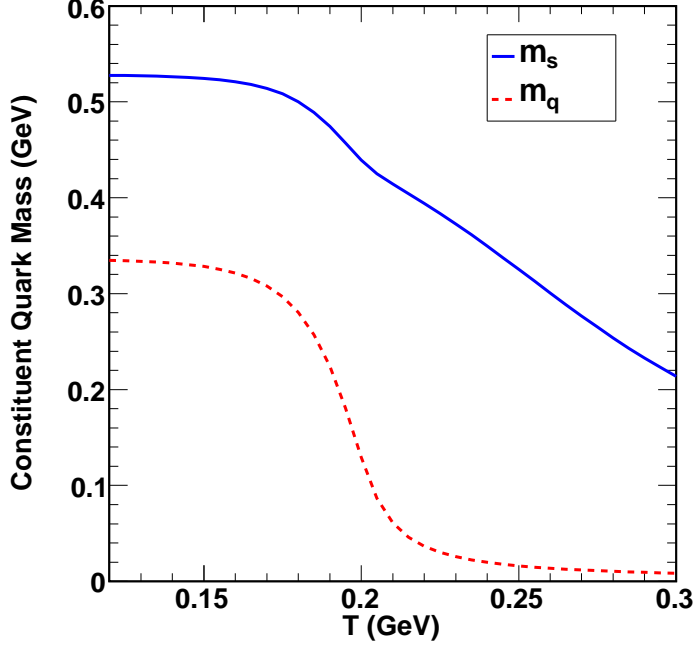


Figure 3. The temperature dependence of the constituent quark masses, m_q and m_s , in (7) and (8) respectively.

$$n_{\bar{q}} = n_{\bar{u}} + n_{\bar{d}} = 4N_c \int \frac{d^3k}{(2\pi)^3} f_{\bar{q}}(k), \quad (22)$$

$$n_{q-\bar{q}} = n_q - n_{\bar{q}} = 4N_c \int \frac{d^3k}{(2\pi)^3} [f_q(k) - f_{\bar{q}}(k)], \quad (23)$$

$$n_g = 2(N_c^2 - 1) \int \frac{d^3k}{(2\pi)^3} f_g(k), \quad (24)$$

where the momentum integration is taken without imposing any cutoff. The number of flavors in (21)-(23) is 2 because we are evaluating the quark, antiquark, or net quark number densities for flavor u and d . Figure 6(a) shows the temperature dependence of the (scaled) quark, antiquark, net quark and gluon number densities, n_q/T^3 , $n_{\bar{q}}/T^3$, $n_{q-\bar{q}}/T^3$ and n_g/T^3 , respectively. In figure 6(a), $n_{q-\bar{q}}/T^3$ possesses similar features as that in the two-flavor PNJL model [13]. Moreover, n_g/T^3 is non-vanishing at low temperature due to the existence of the color-singlet gluon states. On the other hand, assuming zero quark chemical potentials for all three flavors, $\mu = \mu_s = 0$, we evaluate n_q/T^3 , n_g/T^3 and the (scaled) strange quark number density n_s/T^3 as functions of the temperature, as shown in figure 6(b). We note that at $T = 1.5T_c$ the quark densities have reached almost 90% of their asymptotic values; whereas the gluon density is still less than 2/3 of its asymptotic value ($n_g/T^3 \approx 1.95$). The quark and gluon number densities reach 99% and 92% of their asymptotic values respectively at $T = 3.5T_c$.

With $f_g(k)$, we can now calculate the contribution of the thermal (transverse)

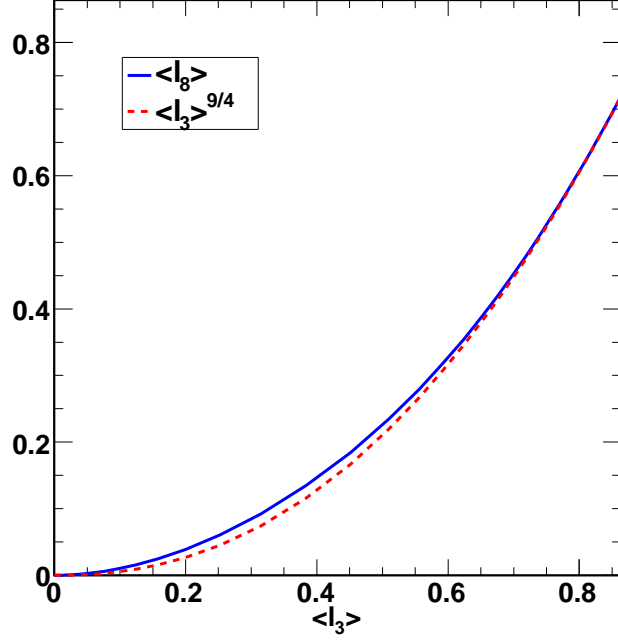


Figure 4. The relations of $\langle \ell_8 \rangle$ to $\langle \ell_3 \rangle$ and $\langle \ell_3 \rangle^{9/4}$ to $\langle \ell_3 \rangle$. The temperature T ranges from 0.12 GeV to 0.30 GeV. These two curves indicates that the values of $\langle \ell_8 \rangle$ and $\langle \ell_3 \rangle$ is consistent with Casimir scaling, $\langle \ell_8 \rangle = \langle \ell_3 \rangle^{9/4}$.

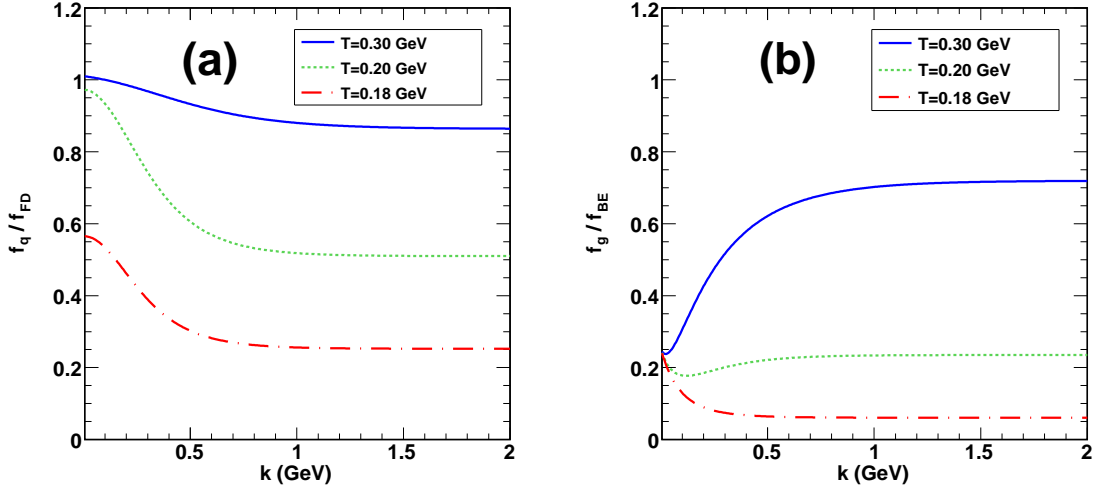


Figure 5. Ratios of distribution functions, (a) $f_q(k)/f_{FD}(k)$, with u and d quark chemical potential $\mu = 0.1$ GeV, and (b) $f_g(k)/f_{BE}(k)$, at temperatures, $T = 0.3, 0.2$ and 0.18 GeV.

gluons to the thermodynamic pressure:

$$p_g = \frac{2(N_c^2 - 1)}{3} \int \frac{d^3k}{(2\pi)^3} |\mathbf{k}| f_g(k), \quad (25)$$

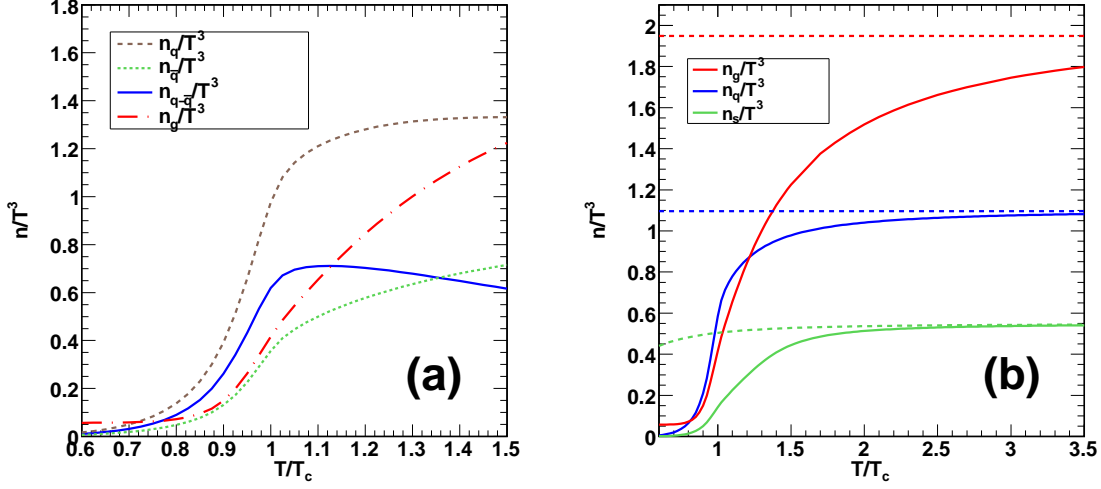


Figure 6. (a) The temperature dependence of the (scaled) quark, antiquark, net quark and gluon number densities, n_q/T^3 , $n_{\bar{q}}/T^3$, $n_{q-\bar{q}}/T^3$ and n_g/T^3 , respectively. The u and d quark chemical potential $\mu = 0.1$ GeV. (b) n_g/T^3 , n_q/T^3 and the (scaled) strange quark number density n_s/T^3 as functions of the temperature, under the assumption of zero quark chemical potentials for all three flavors, $\mu = \mu_s = 0$. In (b), the three dashed curves represent asymptotic values of n_g/T^3 , n_q/T^3 and n_s/T^3 respectively, for $\langle \ell_3 \rangle = \langle \bar{\ell}_3 \rangle = \langle \ell_8 \rangle = 1$ and the current quark masses.

The (scaled) pressure p_g/T^4 is plotted as a function of the temperature in figure 7. Because the thermal average of the adjoint Polyakov loop $\langle \ell_8 \rangle \rightarrow 1$ for $T \gg T_c$, p_g/T^4 approaches the asymptotic behavior predicted by the Stefan-Boltzmann value, $p_g/T^4 \xrightarrow{T \rightarrow \infty} 16\pi^2/90 \approx 1.75$ when $T \gg T_c$. Figure 7 confirms that the gluon pressure reaches 95% of the Stefan-Boltzmann value at $T = 700$ MeV.

4. Strange quark pair-production rate

With the expressions for $f_q(k)$, $f_{\bar{q}}(k)$ and $f_g(k)$, the strange quark pair-production rate for both $q\bar{q} \rightarrow s\bar{s}$ and $gg \rightarrow s\bar{s}$ can be derived in the PNJL model. The strange quark pair-production rate per unit volume is given by

$$A = \frac{dN}{dt d^3x} = A_q + A_g, \quad (26)$$

where

$$A_q = \frac{1}{2} \int_{4m_s^2}^{\infty} ds s \sqrt{1 - \frac{4m_q^2}{s}} \delta(s - (k_1 + k_2)^2) \bar{\sigma}_{q\bar{q} \rightarrow s\bar{s}}(s) \times \int \frac{d^3k_1}{(2\pi)^3 E_q(\mathbf{k}_1)} \int \frac{d^3k_2}{(2\pi)^3 E_q(\mathbf{k}_2)} (2 \times 36) f_q(k_1) f_{\bar{q}}(k_2), \quad (27)$$

$$A_g = \frac{1}{2} \int_{4m_s^2}^{\infty} ds s \delta(s - (k_1 + k_2)^2) \bar{\sigma}_{gg \rightarrow s\bar{s}}(s) \times \int \frac{d^3k_1}{(2\pi)^3 |\mathbf{k}_1|} \int \frac{d^3k_2}{(2\pi)^3 |\mathbf{k}_2|} \left(\frac{1}{2} \times 256\right) f_g(k_1) f_g(k_2), \quad (28)$$

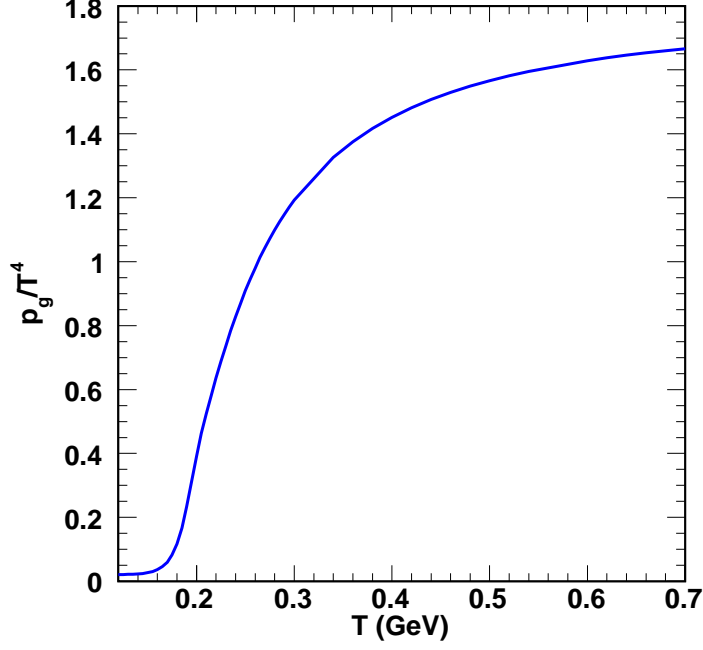


Figure 7. The temperature dependence of the (scaled) thermodynamic pressure, p_g/T^4 , contributed by the thermal (transverse) gluons.

where $E_q(\mathbf{k}) = (|\mathbf{k}|^2 + m_q^2)^{1/2}$. The cross sections are explicitly given by

$$\begin{aligned} \bar{\sigma}_{q\bar{q} \rightarrow s\bar{s}}(s) &= \frac{8\pi\alpha_s^2}{27s^3} \left(s^2 + 2s(m_q^2 + m_s^2) + 16m_q^2m_s^2 \right) \\ &\quad \times \left(1 - \frac{4m_s^2}{s} \right)^{1/2} \left(1 - \frac{4m_q^2}{s} \right)^{-1/2}, \end{aligned} \quad (29)$$

$$\begin{aligned} \bar{\sigma}_{gg \rightarrow s\bar{s}}(s) &= \frac{2\pi\alpha_s^2}{3s} \left\{ \left(1 + \frac{4m_s^2}{s} + \frac{m_s^4}{s^2} \right) \tanh^{-1} \left[\left(1 - \frac{4m_s^2}{s} \right)^{1/2} \right] \right. \\ &\quad \left. - \left(\frac{7}{8} + \frac{31m_s^2}{8s} \right) \left(1 - \frac{4m_s^2}{s} \right)^{1/2} \right\}. \end{aligned} \quad (30)$$

Setting $k_1 = |\mathbf{k}_1|$ and $k_2 = |\mathbf{k}_2|$, we can simplify (27) and (28) as follows:

$$\begin{aligned} A_q &= \frac{9}{4\pi^4} \int_{4m_s^2}^{\infty} ds s \sqrt{1 - \frac{4m_q^2}{s}} \bar{\sigma}_{q\bar{q} \rightarrow s\bar{s}}(s) \int_0^{\infty} dk_1 dk_2 \frac{k_1 k_2}{E_q(k_1) E_q(k_2)} \\ &\quad \times \theta \left[2(k_1 k_2 + E_q(k_1) E_q(k_2) + m_q^2) - s \right] f_q(k_1) f_{\bar{q}}(k_2), \end{aligned} \quad (31)$$

$$A_g = \frac{4}{\pi^4} \int_{4m_s^2}^{\infty} ds s \bar{\sigma}_{gg \rightarrow s\bar{s}}(s) \int_0^{\infty} dk_1 dk_2 \theta(4k_1 k_2 - s) f_g(k_1) f_g(k_2). \quad (32)$$

By substituting equations (10), (11), (16), (29) and (30) into equations (31) and (32), the numerical values of the production rates are obtained as functions of the temperature.

Figure 8 shows the temperature dependence of the strange quark pair-production rates in the PNJL model, compared with those obtained for free quarks. One notices a

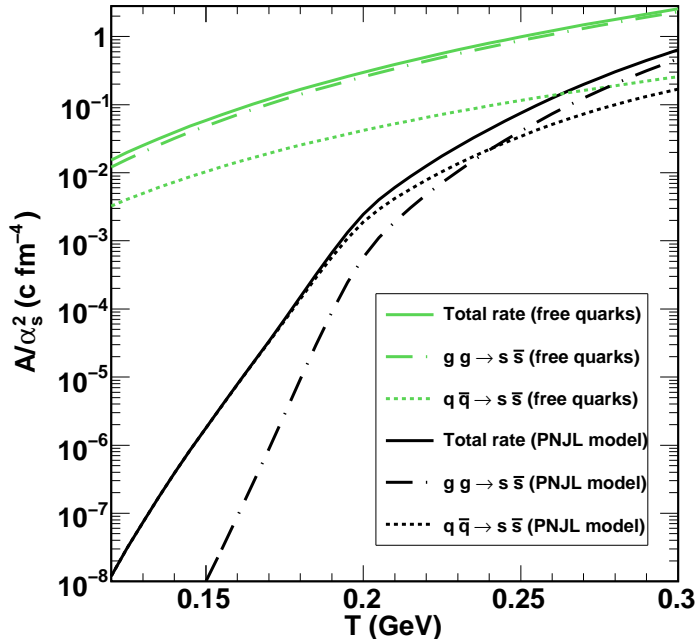


Figure 8. Strange quark pair-production rates divided by α_s^2 as functions of the temperature. The chemical potential for u and d quarks is $\mu = 0.1$ GeV.

number of qualitative differences between the rates calculated in the the PNJL model and those calculated in free perturbation theory. First, the rates are suppressed for all values of the temperature. This is, in part, due to the suppression of the thermal quark- and gluon excitations by the Polyakov loop and, in another part, due to the fact that the effective strange quark mass remains larger than the current quark mass even at temperatures moderately above T_c , as shown in figure 3. We also note that the curves for the Polyakov loop-suppressed gluon induced production rate A_g drops below the quark induced production rate A_q below $T \approx 240$ MeV, reflecting the stronger suppression of gluons at low temperature caused by the Casimir scaling of the thermal average of the adjoint Polyakov loop.

5. Conclusions

We have studied the effects of deconfinement and chiral symmetry breaking on the rates of strange quark pair production in the framework of the PNJL model. As proposed in [2, 4], the strange quark pair-production rate is enhanced in the deconfined phase for the free quarks and the production rate for $gg \rightarrow s\bar{s}$ is dominant at all temperatures. In the PNJL model, the enhanced production of strange quarks is also obtained, but the production rates for $q\bar{q} \rightarrow s\bar{s}$ and $gg \rightarrow s\bar{s}$ cross over at $T_r \approx 240$ MeV. The production rate for $q\bar{q} \rightarrow s\bar{s}$ is dominant when $T < T_r$, while that for $gg \rightarrow s\bar{s}$ is dominant when $T > T_r$. Besides, when $T < T_c$, the production rates for $q\bar{q} \rightarrow s\bar{s}$ and $gg \rightarrow s\bar{s}$ are

both very small in the PNJL model because quark and gluon quasiparticles are strongly suppressed below T_c . In this temperature region, strangeness production is dominated by hadronic reactions, which were investigated by Rehberg *et al.* in the NJL model [20].

In figure 8, the coupling α_s scales out when we compare the quark and gluon contributions to the production rate. We note that, approaching T_c , one needs to take into account the interactions originated from the appearance of collective modes due to the onset of the spontaneous breaking of chiral symmetry, rendering our treatment incomplete in the transition region. However, our goal was to study at what temperature above T_c the gluonic contribution to the production rate becomes dominant. We found that this temperature is around 240 MeV within the framework of the PNJL model. Because this threshold is well beyond the temperature range in which the chiral phase transition occurs, as can be seen from figure 2, our neglect of the contribution from collective (hadronic) modes appears justified.

A by-product of our investigation is the demonstration that the thermal average in (18) satisfies Casimir scaling (20) of the fundamental and adjoint Polyakov loops. This gives confidence that the weight function (19) can be used to obtain the temperature dependence of any quantity that involves the eigenvalues of the Polyakov loop. For example, the temperature dependence of $f_g(k)$ requires the evaluation of the averages $\langle \text{tr}_A L_8^n \rangle$. In turn, $f_g(k)$ makes it possible to compute the contribution of the thermal (transverse) gluons to the pressure as a function of the temperature. This makes it unnecessary to include this contribution explicitly in the effective potential for the Polyakov loop, as sometimes done in the literatures [13, 21].

In our study, the phase transformations of QCD, including deconfinement and chiral symmetry breaking, are incorporated into the evaluation of the thermal strange quark pair-production rate. Using the same techniques, the effects of the Polyakov loop on other signatures of quark-gluon plasma can be explored in the future.

Acknowledgements

This work was supported in part by the U. S. Department of Energy under grant DE-FG02-05ER41367. We thank Kenji Fukushima for several enlightening discussions about the PNJL model. We thank Inga Kouznetsova for helpful advice and Johann Rafelski for comments on the draft of this manuscript. One of us (BM) acknowledges the hospitality and support of the Yukawa Institute for Theoretical Physics in Kyoto during the workshop program entitled *New Frontiers in QCD 2008*, which motivated this work.

Appendix A. Averaging procedures

In this section, we discuss several Polyakov-loop averaging procedures for the grand canonical thermodynamic potential in the quark sector and study their implications for the quark and antiquark distribution functions. This study can be easily extended to

the Polyakov-loop averaging procedures in the gluon thermodynamic potential, which are not explicitly formulated here. The quark grand canonical thermodynamic potential per unit volume is defined in terms of the quark grand partition function,

$$\Omega_q = -\frac{T}{V} \ln \langle Z \rangle, \quad (\text{A.1})$$

where V denotes the volume of the system. In the mean-field approximation, the quark grand partition function is associated with a set of quantum numbers, $\alpha = \{\mathbf{k}, s, f, c, \pm\}$, where \mathbf{k} , s , f , c and \pm denotes momentum, spin, flavor, color and particle/antiparticle quantum number respectively. The average in (A.1) is taken over the eigenvalues of the Polyakov loop, as shown explicitly in (18). Instead of the full average used in (A.1), an approximate averaging method used more frequently in the PNJL model is the quenched average:

$$\Omega_q \approx -\frac{T}{V} \langle \ln Z \rangle = -\frac{T}{V} \langle \ln \det Z_\alpha \rangle, \quad (\text{A.2})$$

where Z_α denotes the single-particle partition function for each quantum number and the determinant runs over all quantum numbers α . Various further approximations can be applied to (A.2), which entail distinct averaging procedures. In the following texts, we discuss the differences among several Polyakov-loop averaging procedures for the quark thermodynamic potential and clarify their effects on the quark and antiquark distribution functions.

Define the following subsets of α : $\bar{\alpha} = \{\mathbf{k}, s, f, \pm\}$, $\bar{\alpha}_1 = \{\mathbf{k}, s, f\}$ and $\bar{\alpha}_2 = \{\pm\}$. Starting from (A.2), we have the following (approximate) averaging procedures:

$$\Omega_q \approx -\frac{T}{V} \sum_{\bar{\alpha}} \ln \left\langle \det_c Z_{\bar{\alpha},c} \right\rangle, \quad (\text{A.3})$$

$$\bar{\Omega}_q \approx -\frac{T}{V} \sum_{\bar{\alpha}} \left\langle \ln \det_c Z_{\bar{\alpha},c} \right\rangle, \quad (\text{A.4})$$

$$\hat{\Omega}_q \approx -\frac{T}{V} \sum_{\bar{\alpha}_1} \ln \left\langle \prod_{\bar{\alpha}_2} \det_c Z_{\bar{\alpha}_1, \bar{\alpha}_2, c} \right\rangle, \quad (\text{A.5})$$

where \det_c denotes the color determinant. Equation (A.3) is the Weiss mean-field approximation, which is frequently used in the literatures of the PNJL model [11, 13]. We note that (A.3) and (A.4) take the Polyakov-loop average for quarks and antiquarks separately. This implies that, in the limit $\langle \text{tr}_F L_3 \rangle \rightarrow 0$, only states with baryon quantum (quark-triplet) numbers contribute, but not states with meson quantum numbers (quark-antiquark pairs). We further note that (A.3) and (A.5) replace the quenched average over the Polyakov loop configuration by the unquenched average. We compare Ω_q with $\bar{\Omega}_q$ in Appendix A.1 and Ω_q with $\hat{\Omega}_q$ in Appendix A.2. respectively, by deriving the quark distribution functions from equations (A.3)-(A.5).

Appendix A.1. Validity of the Weiss mean-field approximation

By the averaging procedure in (A.3), the quark thermodynamic potential per unit volume in (6) is simplified to be

$$\begin{aligned} \Omega_q = & -2T \sum_{f=u,d,s} \int \frac{d^3k}{(2\pi)^3} \left\{ \ln \left[1 + 3\langle \ell_3 \rangle \lambda_+ + 3\langle \bar{\ell}_3 \rangle \lambda_+^2 + \lambda_+^3 \right] \right. \\ & \left. + \ln \left[1 + 3\langle \bar{\ell}_3 \rangle \lambda_- + 3\langle \ell_3 \rangle \lambda_-^2 + \lambda_-^3 \right] \right\} \\ & - 6 \sum_{f=u,d,s} \int \frac{d^3k}{(2\pi)^3} E_f(\mathbf{k}) \theta(\Lambda^2 - |\mathbf{k}|^2), \end{aligned} \quad (\text{A.6})$$

where $\lambda_{\pm} = \exp[-(|\mathbf{k}|^2 + m_q^2)^{1/2} \mp \mu]/T$. The quark and antiquark distribution functions, (10) and (11), are easily obtained from (A.6). On the other hand, if we start from (6) and use the averaging procedure defined in (A.4), the quark and antiquark distribution functions are alternatively obtained:

$$\bar{f}_q(k) = \left\langle \frac{\ell_3 \lambda_+ + 2\bar{\ell}_3 \lambda_+^2 + \lambda_+^3}{1 + 3\ell_3 \lambda_+ + 3\bar{\ell}_3 \lambda_+^2 + \lambda_+^3} \right\rangle, \quad (\text{A.7})$$

$$\bar{f}_{\bar{q}}(k) = \left\langle \frac{\bar{\ell}_3 \lambda_- + 2\ell_3 \lambda_-^2 + \lambda_-^3}{1 + 3\bar{\ell}_3 \lambda_- + 3\ell_3 \lambda_-^2 + \lambda_-^3} \right\rangle, \quad (\text{A.8})$$

where ℓ_3 and $\bar{\ell}_3$ are expressed in (13). By the definition of the thermal average (18) and the weight function (19), we can evaluate (A.7) and (A.8) explicitly. Without losing generality, in this section we assume a vanishing u and d quark chemical potential, i.e. $\mu = 0$, which implies the simplification $\langle \bar{\ell}_3 \rangle = \langle \ell_3 \rangle$. Figure A1(a) shows the comparison of the ratio $f_q(k)/f_{\text{FD}}(k)$ obtained from (10) with the ratio $\bar{f}_q(k)/f_{\text{FD}}(k)$ from (A.7). The figure shows that the two ratios agree well for all temperatures, especially in the high momentum region, which is most relevant for the thermal strange quark pair-production rate.

The gluon distribution function in (16) is derived from the gluon thermodynamic potential obtained by the averaging procedure analogous to (A.4). On the other hand, if using the averaging procedure analogous to (A.3) instead, we obtain the gluon distribution function under the Weiss mean-field approximation, namely

$$f_g(k) \approx \frac{\frac{1}{8} \langle \text{tr}_A L_8 \rangle \exp(-|\mathbf{k}|/T)}{1 - \frac{1}{8} \langle \text{tr}_A L_8 \rangle \exp(-|\mathbf{k}|/T)}, \quad (\text{A.9})$$

assuming

$$\langle \text{tr}_A L_8^n \rangle \approx 8 \left(\frac{1}{8} \langle \text{tr}_A L_8 \rangle \right)^n. \quad (\text{A.10})$$

Figure A1(b) shows the comparison of the ratio $f_g(k)/f_{\text{BE}}(k)$ obtained from (A.9) with that from (16). They agree well in the high momentum region but deviate in the low momentum region.

Appendix A.2. Alternative quark and antiquark distribution functions

By the Polyakov-loop averaging procedure (A.5), we evaluate alternative quark and antiquark distribution functions, which, unsurprisingly, incorporate the probabilities of

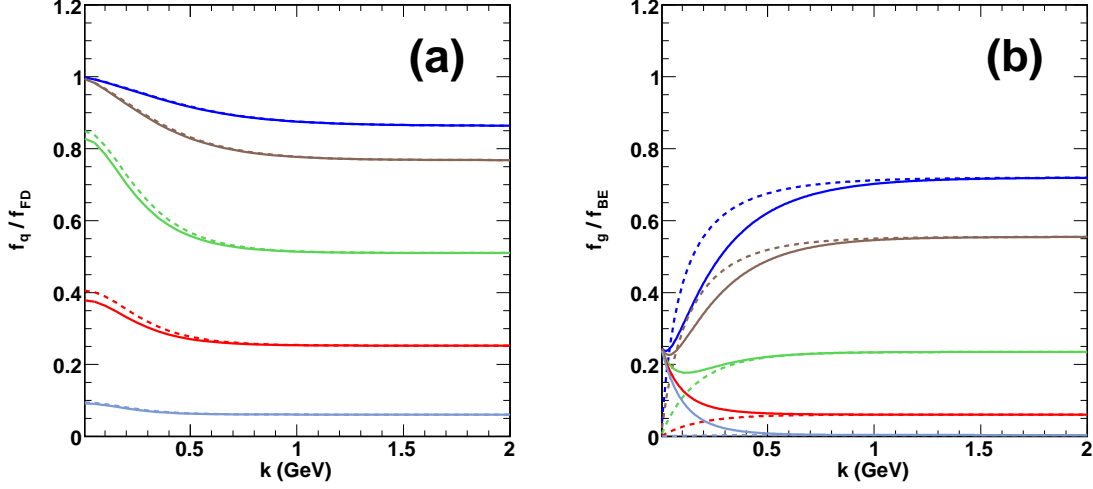


Figure A1. Validity of the Weiss approximation for, (a) $f_q(k)/f_{\text{FD}}(k)$, assuming a zero quark chemical potential, and (b) $f_g(k)/f_{\text{BE}}(k)$. The solid curves denote the ratios obtained by, (a) $\hat{f}_q(k)/f_{\text{FD}}(k)$, where $\hat{f}_q(k)$ is defined in (A.7) with $\mu = 0$, and (b) $f_g(k)/f_{\text{BE}}(k)$, where $f_g(k)$ is defined in (16). The dashed curves denote the ratios obtained by, (a) $f_q(k)/f_{\text{FD}}(k)$, where $f_q(k)$ defined in (10) with $\mu = 0$ and $\langle \bar{\ell}_3 \rangle = \langle \ell_3 \rangle$, and (b) $f_g(k)/f_{\text{BE}}(k)$, where $f_g(k)$ defined in (A.9). The curves are obtained at temperatures, $T = 0.3, 0.25, 0.2, 0.18$ and 0.15 GeV (top to bottom).

color-singlet quark-antiquark states. The quark distribution function derived from the averaging procedure (A.5) is

$$\begin{aligned}
\hat{f}_q(k) = & \frac{1}{3} \left[3e^{-\frac{6E_q(k)}{T}} + 3\langle \text{tr}_F L_3 \rangle e^{-\frac{(5E_q(k)-\mu)}{T}} + 2\langle \text{tr}_F L_3^\dagger \rangle e^{-\frac{(5E_q(k)+\mu)}{T}} \right. \\
& + 2\langle \text{tr}_F L_3 \text{tr}_F L_3^\dagger \rangle e^{-\frac{4E_q(k)}{T}} + 3\langle \text{tr}_F L_3^\dagger \rangle e^{-\frac{(4E_q(k)-2\mu)}{T}} \\
& + \langle \text{tr}_F L_3 \rangle e^{-\frac{(4E_q(k)+2\mu)}{T}} + 2(2\langle \text{tr}_F L_3 \rangle + \langle \text{tr}_F (L_3^\dagger)^2 \rangle) e^{-\frac{(3E_q(k)-\mu)}{T}} \\
& + (2\langle \text{tr}_F L_3^\dagger \rangle + \langle \text{tr}_F L_3^2 \rangle) e^{-\frac{(3E_q(k)+\mu)}{T}} + \langle \text{tr}_F L_3 \text{tr}_F L_3^\dagger \rangle e^{-\frac{2E_q(k)}{T}} \\
& \left. + 3e^{-\frac{3(E_q(k)-\mu)}{T}} + 2\langle \text{tr}_F L_3^\dagger \rangle e^{-\frac{2(E_q(k)-\mu)}{T}} + \langle \text{tr}_F L_3 \rangle e^{-\frac{(E_q(k)-\mu)}{T}} \right] \\
& \times \left[1 + e^{-\frac{6E_q(k)}{T}} + \langle \text{tr}_F L_3 \rangle e^{-\frac{(5E_q(k)-\mu)}{T}} + \langle \text{tr}_F L_3^\dagger \rangle e^{-\frac{(5E_q(k)+\mu)}{T}} \right. \\
& + \langle \text{tr}_F L_3 \text{tr}_F L_3^\dagger \rangle e^{-\frac{4E_q(k)}{T}} + \langle \text{tr}_F L_3^\dagger \rangle e^{-\frac{(4E_q(k)-2\mu)}{T}} \\
& + \langle \text{tr}_F L_3 \rangle e^{-\frac{(4E_q(k)+2\mu)}{T}} + (2\langle \text{tr}_F L_3 \rangle + \langle \text{tr}_F (L_3^\dagger)^2 \rangle) e^{-\frac{(3E_q(k)-\mu)}{T}} \\
& + (2\langle \text{tr}_F L_3^\dagger \rangle + \langle \text{tr}_F L_3^2 \rangle) e^{-\frac{(3E_q(k)+\mu)}{T}} \\
& + \langle \text{tr}_F L_3 \text{tr}_F L_3^\dagger \rangle e^{-\frac{2E_q(k)}{T}} + e^{-\frac{3(E_q(k)-\mu)}{T}} + e^{-\frac{3(E_q(k)+\mu)}{T}} \\
& + \langle \text{tr}_F L_3^\dagger \rangle e^{-\frac{2(E_q(k)-\mu)}{T}} + \langle \text{tr}_F L_3 \rangle e^{-\frac{2(E_q(k)+\mu)}{T}} \\
& \left. + \langle \text{tr}_F L_3 \rangle e^{-\frac{(E_q(k)-\mu)}{T}} + \langle \text{tr}_F L_3^\dagger \rangle e^{-\frac{(E_q(k)+\mu)}{T}} \right]^{-1}, \tag{A.11}
\end{aligned}$$

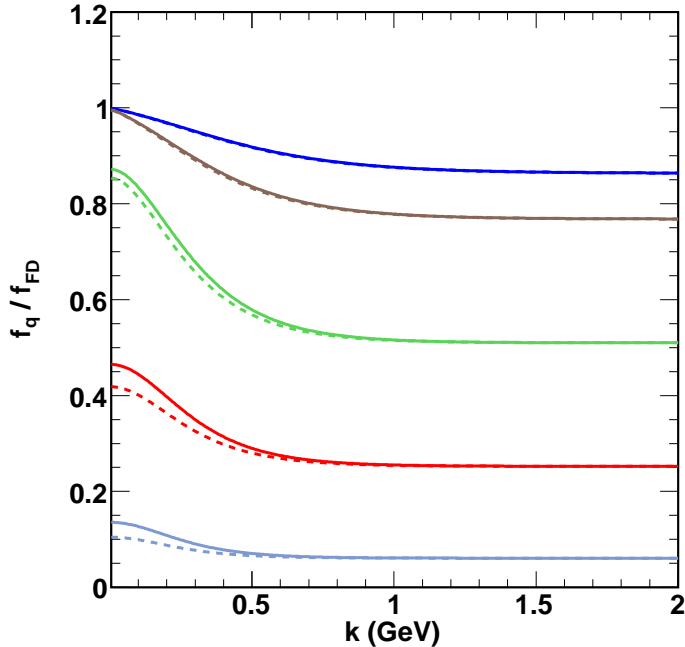


Figure A2. The comparison of the ratio $\hat{f}_q(k)/f_{\text{FD}}(k)$ obtained from (A.11), in solid curves, with $f_q(k)/f_{\text{FD}}(k)$ obtained from (10), in dashed curves, assuming a quark chemical potential $\mu = 0$. The curves are obtained at temperatures, $T = 0.3, 0.25, 0.2, 0.18$ and 0.15 GeV (top to bottom).

where $E_q(k) = (k^2 + m_q^2)^{1/2}$ and $\langle \text{tr}_F L_3 \text{tr}_F L_3^\dagger \rangle = \langle \text{tr}_A L_8 \rangle + 1$. Moreover, the antiquark distribution function $\hat{f}_{\bar{q}}(k)$ can be obtained from (A.11) by interchanging L_3 and L_3^\dagger and replacing μ by $-\mu$. Equation (A.11) contains a sum over the probabilities of all states of N_1 quarks and N_2 antiquarks, where $N_1, N_2 = \{0, 1, 2, 3\}$. As noted before, (A.11) incorporates the contribution of color-singlet quark-antiquark states, which are not contained in the expression (10). Figure A2 shows the comparison of the ratio $\hat{f}_q(k)/f_{\text{FD}}(k)$ obtained from (A.11) with $f_q(k)/f_{\text{FD}}(k)$ obtained from (10), again for $\mu = 0$. The figure shows that the two ratios agree well for all temperatures, especially in the high momentum region. We also note that, when T is near T_c or $T < T_c$, $\hat{f}_q(k)$ in (A.11) is slightly larger than $f_q(k)$ of (10) in the low momentum region. This difference can be traced back to the contribution of the color-singlet quark-antiquark states.

In conclusion, because both $\bar{f}_q(k)$ and $\hat{f}_q(k)$ are in good numerical agreement with $f_q(k)$, we are justified to use (10) and (11) in the evaluation of the strange quark pair-production rate, as done in the main part of this article.

References

- [1] R. Hagedorn and J. Rafelski, Phys. Lett. B **97**, 136 (1980).
- [2] J. Rafelski and B. Müller, Phys. Rev. Lett. **48**, 1066 (1982) [Erratum-ibid. **56**, 2334 (1986)].
- [3] T. S. Biró, B. Lukacs, J. Zimanyi and H. W. Barz, Nucl. Phys. A **386**, 617 (1982).

- [4] P. Koch, B. Müller and J. Rafelski, Phys. Rept. **142**, 167 (1986).
- [5] T. Matsui, B. Svetitsky and L. D. McLerran, Phys. Rev. D **34**, 783 (1986) [Erratum-ibid. D **37**, 844 (1988)].
- [6] E. Andersen *et al.* [WA97 Collaboration], Phys. Lett. B **449**, 401 (1999).
- [7] B. I. Abelev *et al.* [STAR Collaboration], Phys. Rev. C **77**, 044908 (2008).
- [8] M. Kaneta and N. Xu, arXiv:nucl-th/0405068.
- [9] J. Letessier and J. Rafelski, Eur. Phys. J. A **35**, 221 (2008).
- [10] M. Ciminale, R. Gatto, N. D. Ippolito, G. Nardulli and M. Ruggieri, Phys. Rev. D **77**, 054023 (2008).
- [11] K. Fukushima, Phys. Rev. D **77**, 114028 (2008) [Erratum-ibid. D **78**, 039902 (2008)].
- [12] K. Fukushima, Phys. Lett. B **591**, 277 (2004).
- [13] C. Ratti, M. A. Thaler and W. Weise, Phys. Rev. D **73**, 014019 (2006).
- [14] H. Hansen, W. M. Alberico, A. Beraudo, A. Molinari, M. Nardi and C. Ratti, Phys. Rev. D **75**, 065004 (2007).
- [15] P. N. Meisinger, T. R. Miller and M. C. Ogilvie, Phys. Rev. D **65**, 034009 (2002).
- [16] E. Megías, E. Ruiz Arriola and L. L. Salcedo, Phys. Rev. D **74**, 065005 (2006).
- [17] A. Gocksch and M. Ogilvie, Phys. Rev. D **31**, 877 (1985).
- [18] S. Gupta, K. Hübner and O. Kaczmarek, Phys. Rev. D **77**, 034503 (2008).
- [19] S. Gupta, K. Hübner and O. Kaczmarek, Nucl. Phys. A **785**, 278 (2007).
- [20] P. Rehberg, S. P. Klevansky and J. Hüfner, Phys. Rev. C **53**, 410 (1996).
- [21] S. Roessner, C. Ratti and W. Weise, Phys. Rev. D **75**, 034007 (2007).